

# CHARACTERIZATION OF QSPA PLASMA STREAMS IN PLASMA - SURFACE INTERACTION EXPERIMENTS: SIMULATION OF ITER ELMS

V.A. Makhlay

*Institute of Plasma Physics NSC “Kharkov Institute of Physics and Technology”, Kharkov, Ukraine*

*E-mail: makhlay@ipp.kharkov.ua*

Experimental simulations of ITER ELMs with relevant surface heat loads (energy density up to  $2.4 \text{ MJ/m}^2$ ) have been performed with a quasi-steady-state plasma accelerator QSPA Kh-50. Additional shielding effect has been registered during irradiation of the combined carbon–tungsten (C–W) surfaces. Correlation between mass losses and thresholds of erosion products ejection has been analyzed depending on the surface heat loads. For heat load below cracking threshold mass losses are caused by physical spattering. Splashing of liquid material is registered for heat load exceeding the melting threshold.

PACS: 52.40 Hf

## INTRODUCTION

The energy load to plasma facing components (PFCs) during disruptions in ITER are expected in the range of tens of  $\text{GW/m}^2$  with time duration of about 1 ms [1, 2]. In contrast to disruptions that are relatively rare events, type I Edge Localized Modes (ELMs) are anticipated to occur with a frequency of the order of 1 Hz (i.e., few hundred ELMs per ITER pulse). Plasma loads at the tungsten surface for type I ELMs are foreseen to be of  $q = (0.2 \dots 2) \text{ M/Jm}^2$  and the ELM duration of  $t = (0.1 \dots 0.5) \text{ ms}$  [2].

The power loads on current tokamaks associated with the type I ELMs generally do not affect the lifetime of divertor elements. However, the ITER ELMs may lead to unacceptable lifetime [2-5]. Special investigations on material behavior at the ELM relevant loads are thus important. To estimate the range of tolerable loads the effects of ELMs on the lifetime of plasma facing components should be experimentally simulated for large numbers of impacts with varying energy density.

A number of powerful test facilities are available to provide examination of different materials under transient ITER-like loads [5-8]. Among most important tasks for simulation experiments with plasma accelerators are studies of the threshold conditions for cracking of different tungsten grades and issues related to volumetric damages in the course of a large number of exposures, dynamics of evaporated tungsten and penetration of W impurities into plasma (especially for the combination of disruption events with edge-localized modes (ELMs)).

This paper presents the characteristics of QSPA Kh-50 plasma streams and analysis of contribution of different erosion mechanisms to the material damage under plasma heat loads expected for ITER ELMs.

## 1. EXPERIMENTAL SETUP AND DIAGNOSTICS

Experimental simulations of ITER transient events with relevant surface heat load parameters (energy density and the pulse duration) as well as particle loads have been performed with the QSPA Kh-50 quasi-steady-state plasma accelerator, which is the largest and most powerful device of this kind [7, 9]. The main

parameters of QSPA plasma streams were as follows: ion impact energy about  $0.4 \dots 0.6 \text{ keV}$ , the maximum plasma pressure 3.2 bars, and the plasma stream diameter about 18 cm. The surface energy loads were varied in the range of  $(0.1 \dots 1.1) \text{ MJm}^2$  [10, 11]. The plasma pulse shape was approximately triangular, and the pulse duration was about 0.25 ms.

Values of plasma stream energy density were determined on the basis of time resolved measurements of the plasma stream density and its velocity [7, 10, 11]. The energy density in the shielding layer was measured by displacing the calorimeter through a hole in the center of the exposed targets made of tungsten, graphite or combined W-C samples [12]. The calorimeter could be moved into the near-surface plasma up to the distance of 5 cm from the target surface. Observations of plasma interactions with exposed samples, the dust particles dynamics and the droplets monitoring were performed with a high-speed 10 bit CMOS pco.1200 s digital camera PCO AG (exposure time from  $1 \mu\text{s}$  to 1 s, spectral range from 290 to 1100 nm) [10]. A surface analysis was carried out with an MMR-4 optical microscope equipped with a CCD camera.

## 2. EXPERIMENTAL RESULTS

### 2.1. ENERGY DENSITY IN SHIELDING LAYER

The energy density measured in shielding layer by movable calorimeter has been increased with an increasing distance from the target surface (Fig. 1). Afterwards, the energy density reaches saturation at some distance from the surface (2...4) cm, depending on the energy density in the plasma stream) achieving the value of energy density in the incident plasma stream [12]. This allows conclusion that only a part of the plasma jet energy is transferred to the target through the shielding plasma layer.

The energy density absorbed by the tungsten target surface is below 60 % of the QSPA plasma energy density  $q \geq 0.5 \text{ MJ/m}^2$ . This reduction in the energy density is caused by the formation of a dense layer by stopped head part of impacting plasma stream. Such shielding layer protecting the target surface even without evaporation effects is formed during the first instants of the plasma-surface interaction. The plasma density near the target surface achieves  $2 \times 10^{17} \text{ cm}^{-3}$ .

The electron temperature in the near surface layer is practically constant during all period of plasma-surface interaction and it does not exceed 4...5 eV [9, 13].

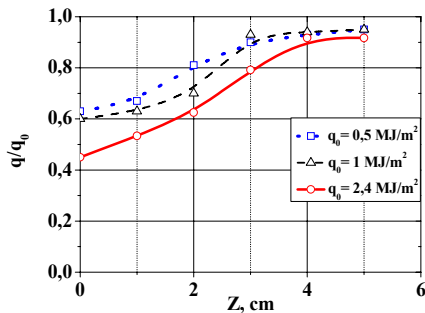


Fig. 1. Ratio of energy density ( $q$ ) in the shielding layer to energy density ( $q_0$ ) of impacting plasma vs. the distance from the target surface ( $Z$ )

Tungsten evaporation onset under the QSPA Kh-50 exposures appears at 1.1  $\text{MJ/m}^2$ . The melting threshold is estimated to be 0.56...0.6  $\text{MJ/m}^2$  [10]. The carbon evaporation threshold is essentially less, being 0.4...0.45  $\text{MJ/m}^2$ . The surface temperature of the graphite target grows with plasma load, reaches a peak value of  $T_s \approx 4000 \text{ K}$  at  $q = 0.45 \text{ MJ/m}^2$  and then remains unaltered with further increase of the plasma load [7]. For combined carbon-tungsten (W-C) targets, W melting and evaporation was not achieved under plasma exposures at a fixed energy density. Additional shielding of the irradiated surface by a C cloud protects W from evaporation even at an essentially increased energy density of impacting plasma (Fig. 2). The fraction of plasma energy, which is absorbed by the target surface, is rapidly decreased with achieving the evaporation onset for exposed targets. At this, the value of heat load to the surface remains practically constant with further increase of the energy density of impacting plasma.

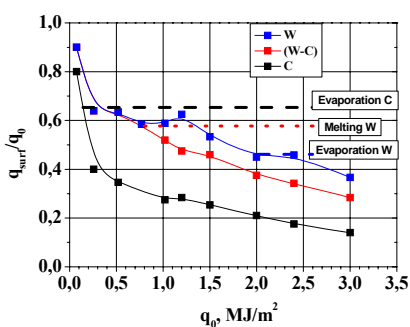


Fig. 2. Ratio of heat load to the target surfaces ( $q_{surf}$ ) to energy density of impacting plasma ( $q_0$ ) vs. the energy density of impacting plasma ( $q_0$ )

## 2.2. MATERIAL EROSION

The irradiation of tungsten surface in QSPA Kh-50 with plasma heat load below the cracking threshold ( $0.3 \text{ MJ/m}^2$ ) does not trigger the generation of erosion products. At the heat load above the cracking threshold but below melting threshold only several dust particles traces have been registered (Fig. 3). Elastic energy

stored in stressed tungsten surface layer should be the motive force for the cracking process with following acceleration of separated solid particles in this case [13, 14].

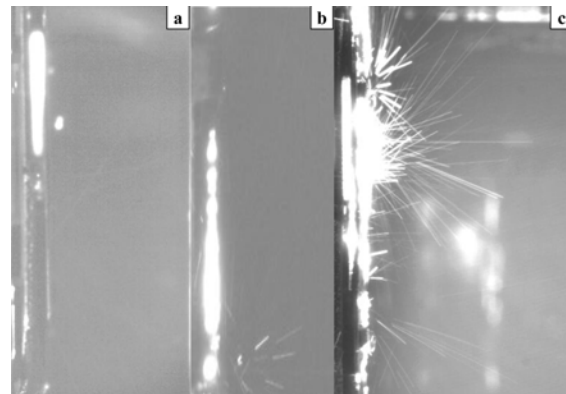


Fig. 3. High speed imaging of plasma interaction with tungsten target:  $t = 1.2 \text{ ms}$  after the start of plasma-surface interaction,  $t_{exp} = 1.2 \text{ ms}$ ; a -  $q_{surf} = 0.45 \text{ MJ/m}^2$ , b -  $q_{surf} = 0.6 \text{ MJ/m}^2$ , c -  $q_{surf} = 0.75 \text{ MJ/m}^2$

Further increase of heat load leads to the surface melting and results in splashing of eroded material. Number of ejected particles rises with increasing heat load due to growing thickness of melt layer. The majority of W particles are ejected from the exposed surface 0.2 ms after beginning of plasma-surface interaction. Maximal velocity of tungsten particles may achieve few tens of m/s [10]. For heat load exceeding the melting threshold, the flying particles can be originated from melt surface due to Kelvin-Helmholtz or Rayleigh-Taylor instabilities [15]. Analysis of obtained experimental results and comparison with the results of numerical simulations [13, 15] allows conclusion that the generation of tungsten particles in the form of droplets may occur only during the plasma pulse and (as latest) few tens microseconds after the pulse end. Other particles may be exclusively solid dust that is generated due to the cracking process under the melt resolidification.

The results of QSPA Kh-50 plasma exposures can be compared with performed experiments on erosion product monitoring in QSPA-T facility [7, 16]. Similar velocity of erosion products and the energy threshold of particles ejection have been observed.

Observations of dust/droplets particles ejected from tungsten are in agreement with measurements of mass losses during high flux irradiation. The average mass loss rate for exposures of  $1.1 \text{ MJ/m}^2$  is about  $(36...40) \mu\text{g cm}^{-2}$  per pulse (Fig. 4). This result correlates with profilometry measurements [9, 7]. The measured value of losses for evaporation onset is 10 times higher than for exposures with a surface load of  $0.75 \text{ MJ/m}^2$  and 25 to 30 times higher than for exposures below the melting threshold. The increase in the mass losses by one order of magnitude is observed with a rise in the target heat load by no more than 50% (from  $0.75$  to  $1.1 \text{ MJ/m}^2$ ). Thus, the boiling essentially adds to the mass losses, possibly due to the intensification of evaporation and the initiation of tungsten splashing.

It should be mentioned that, for heat loads above the melting threshold mass losses periodically fluctuate in accordance with surface evolution of fine intergranular cracks. In this case the corrugation damages will appear for next and next layers, below the surface one. Thus, the consecutive layer by layer erosion will occur [9].

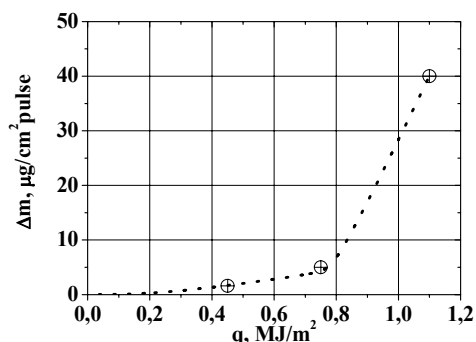


Fig. 4. Dependence of mass loss on applied surface heat load

### CONCLUSIONS

Features of plasma surface interaction and tungsten erosion under repetitive QSPA Kh-50 plasma heat loads, which are relevant to ITER type I ELMs, have been studied. The influence of the neighborhood tungsten and carbon divertor components on the material response to the repetitive plasma heat loads has also been analyzed. Distributions of energy density in shielding layer have been measured as a function of the energy of the incident plasma streams.

Correlation between tungsten mass losses and thresholds of erosion product ejection is analyzed and discussed for different plasma heat loads.

### ACKNOWLEDGEMENTS

This work has been supported in part by IAEA's CRP F1.30.13. The author would like to acknowledge I.E. Garkusha for discussions and interpretation of experimental results as well as the QSPA Kh-50 team for assisting in the experiments.

### REFERENCES

1. G. Federici et al. // *Phys. Scr.* 2006, v. T124, p. 1-8.
2. T. Eich et al. // *J. Nucl. Mater.* 2005, v. 337-339, p. 669.
3. I. Landman et al. // *Phys. Scr.* 2004, v. T111, p. 206.
4. I.E. Garkusha et al. // *J. Nucl. Mater.* 2007, v. 363-365, p. 1021.
5. I.E. Garkusha et al. // *J. Nucl. Mater.* 2009, v. 386-388, p. 127.
6. J. Linke et al. // *J. Nucl. Mater.* 2007, v. 367-370, p. 1422.
7. I.E. Garkusha et al. // *Phys. Scr.* 2009, v. T138, p. 014054.
8. I.E. Garkusha et al. // *Problems of Atomic Science and Technology. Series «Plasma Physics».* 2008, № 6, p. 58-60.
9. V.I. Tereshin et al. // *Plasma Phys. Control. Fusion.* 2007, v. 49, p. A231-A239.
10. I.E. Garkusha et al. // *J. Nucl. Mater.* 2009, v. 337-390-391 p. 814-817.
11. V.A. Makhraj et al. // *Phys. Scr.* 2011, v. T145, p. 014061.
12. A.A. Chuvilo et al. // *Nukleonika.* 2012, v. 57, p. 49.
13. M.S. Ladygina et al. // *Transactions of Fusion Science and technology.* 2011, v. 60, p. 27.
14. S. Pestchanyi et al. // *Phys. Scr.* 2011, v. T145, p. 014062.
15. V.A. Makhraj et al. // *Phys. Scr.* 2019, v. T138, p. 014060.
16. B. Bazylev et al. // *Fus. Eng. and Design.* 2009, v. 84, p. 441.
17. N. Klimov et al. // *J. Nucl. Mater.* 2011, v. 415, p. 559.

Article received 24.01.13

### ОПРЕДЕЛЕНИЕ ХАРАКТЕРИСТИК ПОТОКОВ ПЛАЗМЫ КСПУ В ЭКСПЕРИМЕНТАХ ПО ВЗАИМОДЕЙСТВИЮ ПЛАЗМЫ С ПОВЕРХНОСТЬЮ: МОДЕЛИРОВАНИЕ ELMs В ИТЭРе

В.А. Махлай

Экспериментальное моделирование ELMs в ИТЭРе с соответствующими тепловыми нагрузками на поверхности (плотность энергии до 2.4 МДж/м<sup>2</sup>) было выполнено в квазистационарном плазменном ускорителе КСПУ Х-50. Установлено наличие дополнительного экранирования поверхности при облучении комбинированных углеродно-вольфрамовых поверхностей. Корреляция между потерями массы и порогами инжекции продуктов эрозии была проанализирована в зависимости от величины тепловых нагрузок. При тепловой нагрузке выше порога образования трещин потери массы обусловлены физическим распылением. Разбрызгивание расплавленного материала регистрируется при тепловых нагрузках, превышающих порог плавления.

### ВИЗНАЧЕННЯ ХАРАКТЕРИСТИК ПОТОКІВ ПЛАЗМИ КСПП В ЕКСПЕРИМЕНТАХ ПО ВЗАЄМОДІЇ ПЛАЗМИ З ПОВЕРХНЕЮ: МОДЕЛЮВАННЯ ELMs В ІТЕРі

В.О. Махлай

Експериментальне моделювання ELMs в ІТЕРі з відповідними тепловими навантаженнями на поверхні (густина енергії до 2.4 МДж/м<sup>2</sup>) було виконано в квазістаціонарному плазмовому прискорювачі КСПП Х-50. Встановлено наявність додаткового екранування поверхні при опроміюванні комбінованої вуглецево-вольфрамової поверхні. Кореляція між втратами маси і порогами інжекції продуктів ерозії була проаналізована в залежності від величин теплових навантажень. При тепловому навантаженні вище порогу утворення тріщин втрати маси обумовлені фізичним розпорощуванням. Розбризування розплавленого матеріалу реєструється при теплових навантаженнях, що перевищують поріг плавлення.